Springer

KSME

Journal of Mechanical Science and Technology 24 (8) (2010) 1679~1687
www.springerlink.com/content/1738-494x
DOI 10.1007/s12206-010-0525-y

Effect of rolling ratio on groove-section profile ring rolling †

Yu-Min Zhao* and Dong-Sheng Qian

School of Materials Science and Engineering, Wuhan University of Technology, Wuhan, China

(Manuscript Received January 26, 2010; Revised May 3, 2010; Accepted May 25, 2010)

Abstract

Ring rolling is an advanced plastic forming technique which is used to manufacture precise seamless rings. Rolling ratio is regarded as a decisive parameter for the ring rolling process because it decides the blank dimension, reflects the ring deformation degree and influences the forming results. However, its importance for the ring rolling process is always neglected. In this paper, the effect of rolling ratio on the groove-section profile ring rolling is firstly investigated. The relationships between rolling ratio and blank dimension, rolling ratio and ring deformation degree are theoretically studied and a theoretical value range of rolling ratio is proposed. Then, with FE simulation, the influences of rolling ratio on the forming results are revealed. Based on comparison and experimental verification, a reasonable value range of rolling ratio is determined.

Keywords: Profile ring rolling; Groove-section ring; Rolling ratio; FE simulation

1. Introduction

Ring rolling is an advanced plastic forming technique to cause a ring to reduce its thickness, enlarge its diameter and shape a profile on its surface [1], which is used to manufacture precise seamless rings with various dimensions, shapes and materials. Ring rolling has many advantages such as high productivity, uniform quantity, smooth surface, material saving and it has been used in many industry fields, including aeronautics, astronautics, automobile and atomic energy etc [2].

At present, many research on ring rolling has been carried out by experimental method [3, 4], analytical method [5-7] and finite element method [8-10], which study various aspects like technology design [11, 12], deformation condition [13, 14] and material properties [15]. However, most of the research focused on rectangular section ring rolling and profile ring rolling was rarely investigated, because of the complex deformation rules in profile ring rolling process [16]. A groove-section profiled ring is a typical kind of profiled rings, which is an important part of a ball bearing. Compared with the conventional manufacture methods of groove-section profiled rings like forging, flame cutting, ring rolling shows more economical advantages in productivity improving and material saving. So, in recent years, many attempts have been made at the groove-section profile ring rolling. Hua et al. [17] firstly gave the expression for the motion track of guide roll by analytic calculation. Subsequently, Hua et al. [18] developed a complete 3D FE simulation model to simulate the ring rolling process and testified the model validity by experiment. Hua et al. [19] proposed the plastic penetration condition by FE simulation. Qian et al. [20] investigated the ring gripping condition and its influence factors using statics theory. Qian [21] revealed the movement rules using theoretical calculation and FE simulation. These researches established a theoretical basis for the application and development of groove-section profile ring rolling, but they are still weak to instruct the actual production for lack of the research on technical design.

Rolling ratio is defined as the ratio of the sectional area of blank to that of rolled ring, which is regarded as a decisive parameter for the technical design because it directly influences the blank dimension and ring deformation degree [22]. However, this parameter has not been investigated and its importance for ring rolling is always neglected. So, with no theoretical instruction, the value of rolling ratio is usually selected by repeated rolling experiments, which consume a large amount of materials and time. To focus more attention on rolling ratio, a study for the effect of rolling ratio on groove-section profile ring rolling is firstly carried out.

2. Theoretical analysis

2.1 Working Principle and deformation character of groove-section profile ring rolling

The working principle of groove-section profile ring rolling

† This paper was recommended for publication in revised form by Associate Editor Youngseog Lee

* Corresponding author. Tel.: +86 27 8716 8391, Fax: +86 27 8716 8391
E-mail address: bestcx@yahoo.com.cn

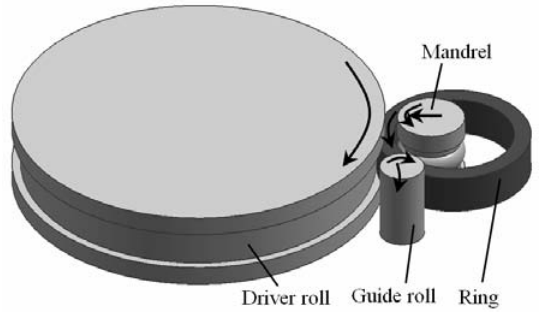

Fig. 1. Schematic illustration of groove-section profile ring rolling.

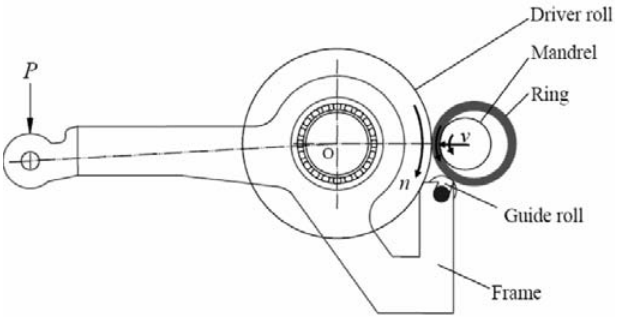

Fig. 2. Schematic diagram of mechanism of guide roll.

is illustrated by Fig. 1. The blank has a rectangular section shape. A closed rolling gap limits the axial spread of the ring and ensures the planeness of the ring end surface. The driver roll takes active rotation. The mandrel is the pressure roll, which takes linear feed motion and passive rotation. The guide roll structure is shown in Fig. 2 [17]. The guide roll fixed on a frame and its center coincides with the center of the driver roll, so it can rotate either around the driver roll center or around the axis of its own. At the end of the frame, a hydraulic cylinder produce a pressure P which makes the guide roll to keep contact with the ring, that help to maintain the stability of ring rolling process and improve the roundness of the rolled ring. In the rolling process, the blank is rolled into the rolling gap repeatedly, one rotation following another, while its thickness is reduced, diameter is enlarged and groove is formed.

Hua et al. [17] indicated that the groove-section profile ring rolling process can be divided into two phases. In the first phase (seen in Fig. 3(a)), the groove ball of mandrel pressing into the ring gradually and the ring groove is mainly formed under the feeding of mandrel, but the ring diameter is less enlarged. In the second phase (seen in Fig. 3(b)), the groove ball of mandrel has pressed into the ring completely and the ring diameter is enlarged adequately under the feeding of mandrel. It can be seen that the process is very complex because the deformation patterns of the ring in the two phases are different.

2.2 Relationship between rolling ratio and blank dimension

The rolling ratio is defined as the ratio of sectional area of blank to that of rolled ring [22], i.e.,

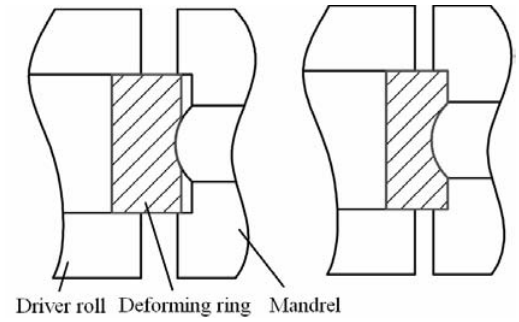

Fig. 3. Two phases of groove-section profile cold ring rolling: (a) the first phase; (b) the second phase.

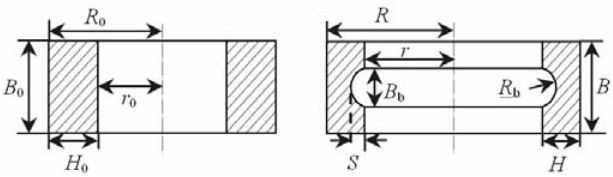

Fig. 4. Ring blank and deformed ring of groove-section profile ring: (a) ring blank; (b) deformed ring.

$$\lambda = \frac{A_0}{A} \tag{1}$$

Fig. 4 shows the dimensions of the blank and rolled ring. According to geometry relationships,

$$A_0 = B_0 H_0$$
$$A = BH + \frac{(R_b - S)B_b}{2} - \arccos\frac{R_b - S}{R_b} R_b^2 \tag{2}$$

The axial width of the ring is approximately changeless because of the axial limitation of the closed rolling gap, so it can be assumed that

$$B_0 = B \tag{3}$$

Substituting Eqs. (2) and (3) into Eq. (1), the expression for H_0 is obtained

$$H_0 = \frac{\lambda A}{B} \tag{4}$$

Allowing for volume conservation in metal plastic deformation, then,

$$\pi(R_0^2 - r_0^2)B_0 = V \tag{5}$$

where V is the volume of rolled ring, which is given by

$$V = \pi B(R^2 - r^2) - 2\pi\left(\frac{B_b k_1}{2} - \frac{B_b^3}{24} + k_2 \arcsin\frac{B_b}{2R_b}\right)$$

$$k_1 = R_b^2 - R_b r + Sr\ ,\ \ k_2 = R_b^2 (r + S - R_b) \tag{6}$$

Substituting Eqs. (4) and (6) into Eq. (5), the relationships between the rolling ratio and the blank dimensions are obtained

$$R_0 = \frac{V}{2\pi\lambda A} + \frac{\lambda A}{2B}\ ,\ \ r_0 = \frac{V}{2\pi\lambda A} - \frac{\lambda A}{2B}\ ,\ \ H_0 = \frac{\lambda A}{B} \tag{7}$$

Performing derivation calculus of Eq. (7) on λ, one has

$$\dot{R}_0 = -\frac{r_0}{\lambda} < 0\ ,\ \ \dot{r}_0 = -\frac{H_0 + r_0}{\lambda} < 0\ ,\ \ \dot{H}_0 = \frac{A}{B} > 0 \tag{8}$$

It can be seen that rolling ratio has decisive effect on blank dimensions. With the increase of rolling ratio, the outer and inner radii of blank decrease, while the radial thickness of blank increases.

2.3 Relationship between rolling ratio and ring deformation degree

The reduction ΔH is used to represent the deformation degree of ring in the rolling process, which is described as

$$\Delta H = \frac{H_0 - H}{H_0} \tag{9}$$

Substituting Eq. (4) into Eq. (9), one has

$$\Delta H = 1 - \frac{BH}{\lambda A} \tag{10}$$

Because the wall thickness of rolled ring is nonuniform, the reductions at the different ring axial locations are different. As seen in Fig. 5, the reductions at the axial locations of CE and GD are the same, whereas the reductions at the axial locations of EG are different, which distribute symmetrically about point F. By calculation, the expression for the average radial thickness of rolled ring is obtained

$$\begin{aligned}\overline{H} &= 2\left(\int_0^{\frac{B_b}{2}} [H - \sqrt{R^2 - y^2} + (R - S)]dy + \int_{\frac{B_b}{2}}^{\frac{B}{2}} H dy\right) / B \\ &= \frac{BH - R^2 \arcsin\frac{B_b}{2R} - \frac{B_b}{4}\sqrt{4R^2 - B_b^{\,2}} + B_b(R - S)}{B}\end{aligned} \tag{11}$$

Then, the maximum reduction, minimum reduction and average reduction are also obtained

$$\Delta H_{\max} = 1 - \frac{B(H - S)}{\lambda A}\ ,\ \ \Delta H_{\min} = 1 - \frac{BH}{\lambda A}\ ,$$
$$\Delta \overline{H} = 1 - \frac{B\overline{H}}{\lambda A} \tag{12}$$

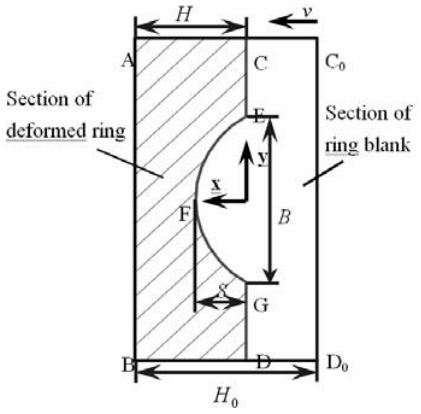

Fig. 5. Reduction calculation o groove-section profile cold ring rolling.

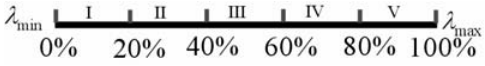

Fig. 6. Five sub-ranges of theoretical value range of rolling ratio.

Eq. (12) illustrates that rolling ratio has directly influence on ring deformation degree. With the increase of rolling ratio, the maximum reduction, minimum reduction and average reduction all increase, thus the ring deformation degree also increases.

2.4 Theoretical value range of rolling ratio

Eq. (8) indicates that the larger the rolling ratio λ, the larger the radial thickness of blank H_0 and the smaller the inner radius of blank r_0, which have some potential disadvantageous effects on the ring rolling process. Hua et al. [11] pointed out that the feed amount per revolution in ring rolling Δh must satisfy the following condition to realize the stable ring rolling process.

$$\begin{aligned}&\Delta h_{\min} \le \Delta h \le \Delta h_{\max} \\ &\Delta h_{\min} = 6.55 \times 10^{-3} H_0^3 \left(\frac{1}{R_1} + \frac{1}{R_2} - \frac{H_0}{R_0 r_0}\right) \\ &\Delta h_{\max} = \frac{2(\arctan\mu)^2 R_1}{(1 + R_1/R_2)^2}\left(1 + \frac{R_1}{R_2} - \frac{R_1 H_0}{R_0 r_0}\right)\end{aligned} \tag{13}$$

where R_1 and R_2 are the working radii of the driver roll and mandrel, respectively; μ is the friction coefficient between the ring and rolls; $\Delta h_{\min}$ is the minimum feed amount per revolution required for the ring plastic penetration condition and $\Delta h_{\max}$ is the maximum feed amount per revolution allowed for the ring gripping condition.

From Eq. (13) it can be seen that with the increase of H_0, $\Delta h_{\min}$ can increase, while $\Delta h_{\max}$ can decrease, thus $\Delta h_{\min}$ may exceed $\Delta h_{\max}$ when H_0 increases to a certain large value with the increasing of λ. So, a large rolling ratio may cause to the unstable deformation of the ring in the rolling process.

Furthermore, the smaller the r_0, the smaller the working ra-

dius of mandrel R_2 and the strength of mandrel is lower, which may easily lead to the mandrel fracture in the rolling process; on the other hand, the larger rolling ratio means the larger deformation in ring rolling process, thus the power consumption is higher and the working life of equipment may decrease under the high load condition in mass production. So, a large rolling ratio is harmful to the working lives of the equipment and mould.

By comparing the production status of various typical rolled rings, Hua [22] summarized that the ring rolling technique is usually used to process the ring with thin wall, of which the thickness is far less than the diameter (usually has $H_0 = 1/2\,R_0 \sim 1/5\,R_0$). So, by referring Hua [22] and above analysis, this paper assumes $H_0 = 1/2\,R_0$ as the ultimate condition for the ring blank satisfied for the stable rolling of groove-section profiled ring. Then, the maximum value condition for the rolling ratio can be defined, that is, the radial thickness of blank is not greater than the inner radius of blank.

$$H_0 \le r_0 \tag{14}$$

Substituting Eq. (7) into Eq. (14), one has

$$\lambda_{\max} \le \sqrt{\frac{VB}{3\pi A^2}} \tag{15}$$

According to the deformation characteristic of ring rolling, The radial thickness of blank must be greater than the maximal radial thickness of rolled ring, which can be defined as the minimum value condition for the rolling ratio, i.e.,

$$\lambda_{\min} > \frac{BH}{A} \tag{16}$$

According to Eq.s (15) and (16), the theoretical value range of rolling ratio is determined

$$\frac{BH}{A} < \lambda \le \sqrt{\frac{VB}{3\pi A^2}} \tag{17}$$

For the convenience of following comparison, the theoretical value range was divided into five sub-ranges, which are called Ⅰ, Ⅱ, Ⅲ, Ⅳ and Ⅴ, respectively, as shown in Fig. 6.

According to Fig. 6, the value ranges of the five sub-ranges are defined as

$$\begin{aligned}
&\text{Ⅰ}.\ \lambda_{\min} - [\lambda_{\min} + 0.2(\lambda_{\max} - \lambda_{\min})] \\
&\text{Ⅱ}.\ [\lambda_{\min} + 0.2(\lambda_{\max} - \lambda_{\min})] - [\lambda_{\min} + 0.4(\lambda_{\max} - \lambda_{\min})] \\
&\text{Ⅲ}.\ [\lambda_{\min} + 0.4(\lambda_{\max} - \lambda_{\min})] - [\lambda_{\min} + 0.6(\lambda_{\max} - \lambda_{\min})] \\
&\text{Ⅳ}.\ [\lambda_{\min} + 0.6(\lambda_{\max} - \lambda_{\min})] - [\lambda_{\min} + 0.8(\lambda_{\max} - \lambda_{\min})] \\
&\text{Ⅴ}.\ [\lambda_{\min} + 0.8(\lambda_{\max} - \lambda_{\min})] - \lambda_{\max}
\end{aligned} \tag{18}$$

3. Comparison with FE simulation

Because above theoretical analysis does not consider the effect of rolling ratio on the forming results, the theoretical value range is wide and imprecise. So, based on the theoretical analysis results, a comparison with FE simulation is carried out to reveal the effect of rolling ratio on the forming results and to determine a precise value range of rolling ratio.

3.1 Key technologies for FE modeling

In the previous works, FE modeling skills for the cold ring rolling process has obtained enough study. Based on the previous research, Hua et al. [19] firstly developed a valid 3D FE simulation model for groove-section profiled ring rolling with the elastic-plastic dynamic explicit FE method. In their research, the FE modeling process was described in detail and the model validity was testified by experiment. So, Based on the ABAQUS CAE software platform, a valid FE model for can be employed in this study by referring to Hua et al. [19]. The key technologies for FE modeling are described briefly as follows.

(1) Cold ring rolling simulation is considered as a quasi-static problem that does not consider the inertial effect during the operation, thus the explicit dynamic finite element procedure is used to avoid the huge computation time and convergence problem of the implicit procedure for the improvement of computational efficiency [13].

(2) Artificially increasing the density of the material, i.e. mass scaling, is a preferred speed-up method [23]. A general rule to obtain an appreciate mass scaling factor, that is, the kinetic energy of deforming material should not exceed a small fraction (typically 5-10%) of its inertial energy throughout most of the process [24]. In this model, the mass scaling factor is defined as 100 to obtain an economical solution.

(3) The rolls and ring are treated as analytical rigid bodies and a deformable body, respectively. Three contact pairs are defined between the ring and the driver roll, mandrel and guide roll, respectively. It is assumed that the friction on the contact surfaces between the ring and the rolls meet the Coulomb friction law and remain unchanged during the whole rolling process.

(4) Because the axial spread of the ring is negligible, the axial constraint is applied to the end surface of the blank, that is, axial displacement of the nodes on the ring end surface is not permitted.

(5) A uniform mesh with an 8-noded first-order reduction integration continuum element (C3D8R) is used. The ALE adaptive remeshing and hourglass control techniques are employed to reduce the mesh distortion and control the zero-energy mode [25].

(6) The motion of the guide roll can be effectively controlled by the method, which was described in detail by Hua et al. [17].

The material of the ring is GCr15 bearing steel. Its density, Young's modulus and Poisson ratio are 7850 $kg.m^{-3}$, 219.1GPa and 0.3, respectively. And its constitutive equation at room temperature is [18]:

$$\begin{cases}\sigma = 219.1\varepsilon^{e}(\text{GPa}) & \varepsilon \le 0.001856 \\ \sigma = [847(\varepsilon^{p})^{0.129} + 30.37](\text{MPa}) & \varepsilon > 0.001856\end{cases}$$

where σ the is true stress, ε^{e} and ε^{p} are the true elastic strain and plastic strain respectively and ε is the true total strain.

The simulative condition is summarized in Table 1. According to Table 1 and Eq. (17), the theoretical value range of rolling ratio is obtained. Taking 0.05 as the interval of the value of λ, the dimensions of the blanks under different values of λ are computed by Eq. (7), as shown in Table 2.

Table 1. Simulative condition.

Parameters		Value
Dimensions of deformed ring	Outer radius/mm	45
	Inner radius/mm	37.175
	Axial height/mm	23.1
	Radius of groove/mm	9
	Radial deepness of groove/mm	2.81
	Axial height of groove/mm	13.067
Dimensions of rolls	Outer radius of driver roll/mm	108.52
	Working radius of driver roll/mm	103.61
	Outer radius of groove ball of mandrel/mm	19.95
	Outer radius of mandrel/mm	19.64
	Working radius of mandrel/mm	17.14
	Working radius of guide roll/mm	13
Forming parameters	Rotational speed of driver roll/r.s-1	2.43
	Feeding speed of mandrel/mm.s-	1
	Friction coefficient	0.15 [26]

Table 2. Dimensions of blanks under different values of λ.

Blank No.	R_0 /mm	r_0 /mm	H_0 /mm	B_0 /mm	λ
1	38.653	30.58	8.073	23.1	1.2
2	37.436	29.027	8.409	23.1	1.25
3	36.326	27.581	8.745	23.1	1.3
4	35.311	26.23	9.081	23.1	1.35
5	34.38	24.962	9.418	23.1	1.4
6	35.525	23.771	9.754	23.1	1.45
7	32.739	22.648	10.091	23.1	1.5
8	32.013	21.586	10.427	23.1	1.55
9	31.344	20.581	10.763	23.1	1.6
10	30.726	19.626	11.1	23.1	1.65
11	30.153	18.717	11.436	23.1	1.7
12	29.623	17.851	11.772	23.1	1.75
13	29.132	17.023	12.109	23.1	1.8
14	28.677	16.231	12.446	23.1	1.85
15	28.254	15.472	12.782	23.1	1.9
16	27.861	14.744	13.118	23.1	1.95
17	27.497	14.043	13.454	23.1	2.0

3.2 Simulative results and discussion

3.2.1 Force and power parameters

The force and power parameters mainly include rolling force and rolling moment. Because the rolling force and rolling moment fluctuate in the whole rolling process, average rolling force $\bar{F}$ and average rolling moment $\bar{M}$ are used for comparison.

Fig. 7 shows the variation curves of $\bar{F}$ and $\bar{M}$ with λ. The average line in the figure represents the average value of the vertical ordinate. It can be seen that $\bar{F}$ and $\bar{M}$ firstly descend, then ascend with the increase of λ.

The rolling force and moment have obvious relations with the feed amount per revolution Δh as the increasing Δh can cause the deformed material per time in the rolling gap to increase, resulting in the rise of deformation resistance, thus the required rolling force and moment can ascend [13]. Hua et al. [11] has given the relationship between Δh and the outer radius of blank R_0, that is

$$\Delta h = \frac{2\pi v R_0}{n_1 R_1} \tag{19}$$

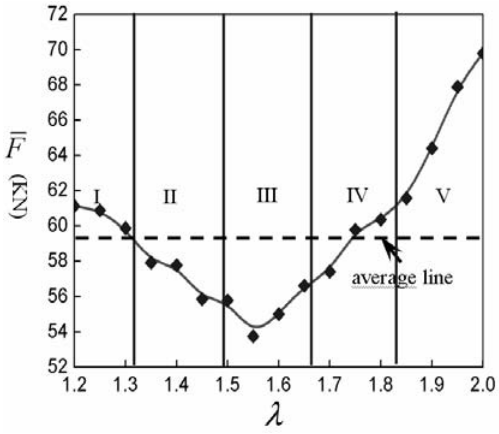

(a)

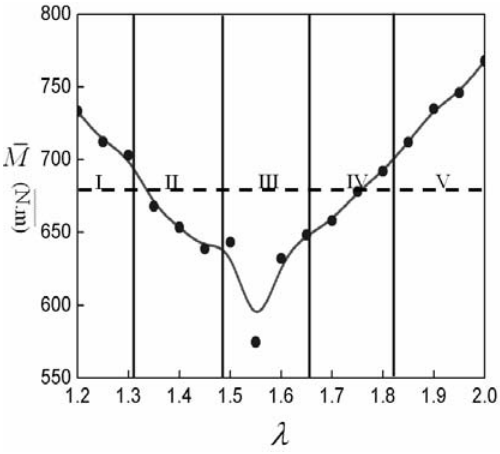

(b)

Fig. 7. Variation curves of $\bar{F}$ and $\bar{M}$ with λ: (a) variation curve of $\bar{F}$ with λ; (b) variation curve of $\bar{M}$ with λ.

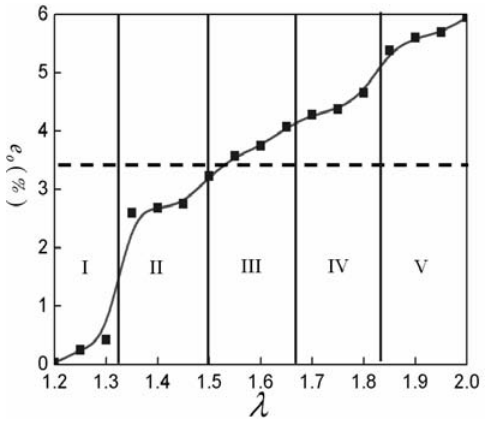

(a)

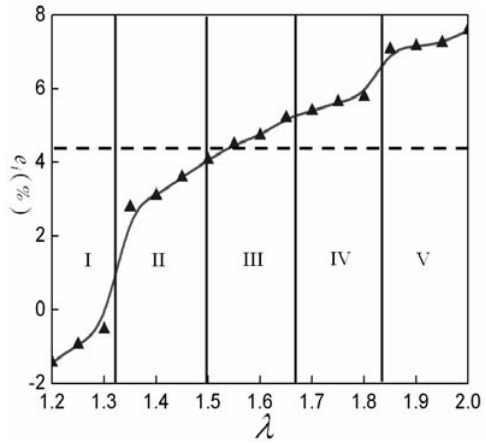

(b)

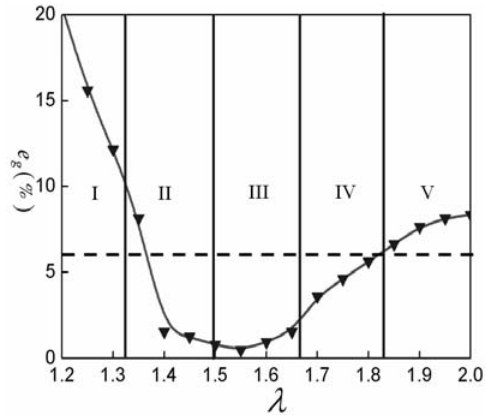

(c)

Fig. 8. Variation curves of e_O, e_i and e_g with λ: (a) variation curve of e_O with λ; (b) variation curve of e_i with λ; (c) variation curve of e_g with λ.

where v is the feeding speed of mandrel, n_1 is the rotational speed of driver roll. So, from Eqs. (8) and (19), it can be seen that with the increase of λ, Δh decreases, the rolling force and moment can descend.

On the other hand, with the increase of λ, the ring deformation degree increases, thus the degree of strain hardening of material increases and the deformation resistance ascends, which can lead to the increase of rolling force and moment. When the increase of λ is less, the change of ring deformation degree is little and the influence of decreasing Δh on the rolling force and moment is dominant; while, when the increase of λ is large, the increase of ring deformation degree is obvious, thus the influence of the increasing ring deformation degree is dominant. So, with the increase of λ, $\bar{F}$ and $\bar{M}$ firstly decrease, then increase.

3.2.2 Geometric accuracy

The geometric accuracy includes the errors of the outer radius of rolled ring e_o, the inner radius of rolled ring e_i and the groove area of rolled ring e_g, which are defined as

$$e_o = \frac{R - R'}{R} \times 100\%, \quad e_i = \frac{r - r'}{r} \times 100\%,$$
$$e_g = \frac{A_g - A'_g}{A_g} \times 100\% \tag{20}$$

where A_g means the groove area of rolled ring, which is described as

$$A_g = \frac{\theta}{180}\pi R_b^2 - (R_b - S)R_b \sin\theta,$$
$$\theta = \arccos\frac{R_b - S}{R_b}R_b^2 \tag{21}$$

and R', r', A'_g mean the simulative values.

Fig. 8 provides the variation curves of e_o, e_i and e_g with λ. It can be seen from Figs. 8(a) and (b) that e_o and e_i increase with the increase of λ, while it can be seen from Fig. 8(c) that e_g firstly descends rapidly, then ascends slowly with the increase of λ.

From above analysis it has been known that Δh can decrease with the increase of λ, so the material in the rolling gap is hard to be penetrated and deform thoroughly with the smaller Δh, which can result in the hard growth of ring diameter. Furthermore, the degree of strain hardening can increase with the increase of λ, thus the material deforms difficultly, which also contribute to the hard growth of ring diameter. So, increasing λ can cause to the increase of e_o and e_i.

Qian [21] has revealed that the deformation rules of ring diameter enlarging and ring groove forming are opposite, that is, the more adequate the ring diameter enlarging, the more insufficient the ring groove forming. However, with the increase of λ, the increasing degree of strain hardening can prevent the material deformation, not only the ring diameter enlarging, but also the groove forming. When the increase of λ is less, the change of ring deformation degree is little, e_g can rapidly decreases with the obvious increase of e_o and e_i; when the increase of λ is large, the increase of ring deformation degree is obvious and the influence of increasing strain hardening on the preventing of groove forming is dominant, thus e_g increases slowly.

The variation laws of e_o, e_i and e_g with λ also validate the previous conclusion that the diameter enlarging and groove forming in groove-section profile ring rolling is asynchronous and interactional. Since the influence of rolling ratio on the ring diameter enlarging is different from that on the ring groove forming, a reasonable rolling ratio must be determined to equilibrate them and obtain the precise rolled ring.

3.2.3 Deformation inhomogeneity

The uniformity of the equivalent plastic stain distribution-SDP is employed to evaluate the deformation inhomogeneity. SDP is defined as [27]

$$\mathrm{SDP}=\sqrt{\sum_{i=1}^{N}((\mathrm{PEEQ}_i-\mathrm{PEEQ}_a)^2.V_i)}\Big/\sum_{i=1}^{N}V_i \tag{22}$$

where $\mathrm{PEEQ}_a=\sum_{i=1}^{N}(\mathrm{PEEQ}_i.V_i)/\sum_{i=1}^{N}V_i$. PEEQ_a is the average equivalent plastic stain (PEEQ), N is the element number of a ring, PEEQ_i is the PEEQ at element i and V_i is the volume of element i.

The larger the SDP value, the more inhomogeneous the ring deformation and the more likely the ring to produce inner flaws and surface cracks.

Fig. 9 describes the variation curve of SDP with λ. It can be seen that SDP evidently increases with the increase of λ. As Δh decreases with the increasing λ, the plastic zone is harder to penetrate the ring wall and the ring deforms more imhomogeneously under the small Δh [22]. Besides, the increasing λ causes to the increase of strain hardening degree of material, the larger the strain hardening degree of material, the more difficultly and inhomogeneously the ring deforms. So, the increasing λ can cause to the evidently increase of SDP.

3.2.4 Processing efficiency

Processing efficiency of a rolled ring is an important index for the productivity of mass production. Using the processing time of one rolled ring T to represent the processing efficiency. Under the uniform feeding speed of mandrel, T can be described as

$$T=\frac{H_0-H}{v}=\frac{\lambda A-BH}{vB} \tag{23}$$

It can be seen from Eq. (23) that for a certain ring product, T is proportional to λ under the same feeding speed. By calculation, the variation curve of T with λ is given by Fig. 10, it can be seen that T linearly increases with the increase of λ.

4. Integrated comparison

Based on the above analysis results, an integrated comparison among the five sub-ranges is performed to determine an optimal value range of rolling ratio, as shown in Table 3.

Table 3. Comparison among the five sub-ranges.

Parameters		Five sub-ranges				
		I	II	III	IV	V
Force and power parameters	rolling force	DAD	AD	AD	DAD	DAD
	rolling moment	DAD	AD	AD	AD	DAD
Geometric accuracy	outer radius	AD	AD	DAD	DAD	DAD
	inner radius	DAD	AD	DAD	DAD	DAD
	groove	DAD	AD	AD	AD	DAD
Deformation inhomogeneity		AD	AD	DAD	DAD	DAD
Processsing efficiency		AD	AD	DAD	DAD	DAD

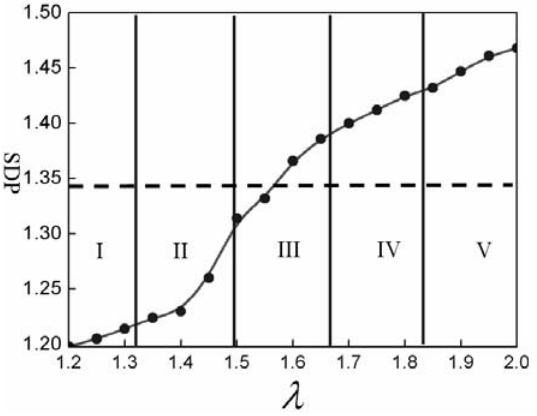

Fig. 9. Variation curve of SDP with λ.

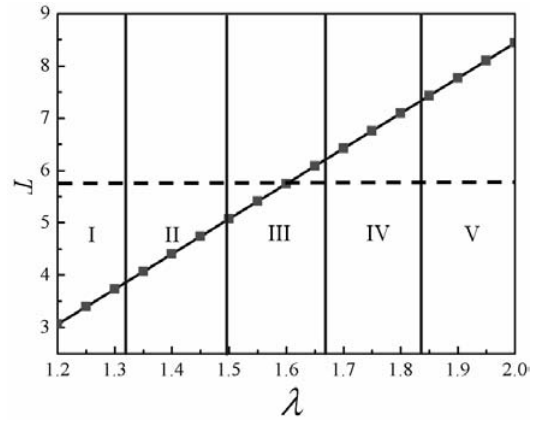

Fig. 10. Variation curve of T with λ.

In Table 3, two indexes are employed to evaluate the effects of five sub-ranges on the forming parameters, which are called AD and DAD, respectively. If the values of one forming parameter within one sub-range are all lower than the average value, AD is selected to represent the advantageous effect of this sub-range on this forming parameter; otherwise, DAD is selected to represent the disadvantageous effect. By compari-

Table 4. Dimension of blanks and rolled rings of four groove-section rings.

Bearing type	Dimensions of deformed ring/mm						Dimensions of ring blank/mm		
	R	r	B	R_b	S	B_b	R_0	r_0	B_0
6308	45	37.175	23.1	9	2.81	13.067	33.75	24	23.1
6306	36.45	29.2	19.9	7.5	1.7	9.51	28.5	20.5	19.9
30TM04	36.1	30.45	22.6	8	1.8	10.111	32.6	23.55	22.6
32TM03	40.62	32.85	24.6	9	2	11.313	34.35	25.1	24.6

Table 5. Actual values and theoretical value ranges of rolling ratios of four groove-section rings.

Bearing type	Actual value of rolling ratio	Theoretical value range				
		Ⅰ	Ⅱ	Ⅲ	Ⅳ	Ⅴ
6308	1.449	1.15-1.32	1.32-1.49	1.49-1.66	1.66-1.83	1.83-2
6306	1.331	1.08-1.23	1.23-1.38	1.38-1.52	1.52-1.67	1.67-1.8
30TM04	1.263	1.08-1.22	1.22-1.37	1.37-1.51	1.51-1.66	1.66-1.8
32TM03	1.279	1.09-1.24	1.24-1.39	1.39-1.55	1.55-1.7	1.7-1.86

son, it can be seen that the number of AD in column of sub-range Ⅱ is the largest, this means that sub-range Ⅱ is the optimal value range.

To evaluate above conclusion, some actual production data for groove-section profile ring rolling were collected, as shown in Table 4.

Table 4 shows the dimensions of blanks and rolled rings of the outer rings of four kinds of groove ball bearings, which are manufactured by Huangshi Hatebeier Precision Forging Co., Ltd., China. According to Table 4, the actual values and theoretical value ranges of the rolling ratios of the four groove0section rings are calculated, as shown in Table 5.

It can be seen from Table 5 that the actual rolling ratios of the four rings are within the sub-ranges Ⅱ of the four theoretical value ranges, respectively. This result validates the conclusion effectively. So, based on the comparison and production verification, the optimal value range of the rolling ratio can be determined, that is

$$\frac{0.8BH}{A}+0.2\sqrt{\frac{VB}{3\pi A^2}}\le\lambda\le\frac{0.6BH}{A}+0.4\sqrt{\frac{VB}{3\pi A^2}} \tag{24}$$

5. Conclusions

In this paper, the influence of rolling ratio on the groove-section profile ring rolling is investigated by theoretical analysis and FE simulation. The research results show that changing rolling ratio causes to the changes of feed amount per revolution in the rolling process and strain hardening degree of material, the two changes are caused by the decisive effects of rolling ratio on the blank geometry and ring deformation degree, respectively. And the two changes are represented by the variation of forming results like rolling force and moment, geometric accuracy, deformation inhomogeneity and processing efficiency under different rolling ratios, i.e., with the increase of rolling ratio, the rolling force and moment firstly descend, then ascend; the errors of outer and inner diameters of the rolled ring increase and the error of groove area of the rolled ring firstly decreases, then increases; the deformation inhomogeneity of the rolled ring increases; the processing efficiency linearly increases. By comparing, a reasonable value range of rolling ratio is determined for equilibrating above variations and its validity is testified by actual production.

Acknowledgments

The work was supported by a grant from the Important National Science & Technology Specific Projects (No. 2009ZX04014-074) and a grant from the National High Technology Research and Development Program of China (863Program) (No. 2009AA04Z112), The supports are gratefully acknowledged.

Nomenclature

λ : Rolling ratio
A_0 : Sectional area of blank
A : Sectional area of rolled ring
R_0 : Outer radius of blank
r_0 : Inner radius of blank
H_0 : Radial thickness of blank
B_0 : Axial width of blank
V : Volume of rolled ring
$\bar{H}$: Average radial thickness of rolled ring
R : Outer radius of rolled ring
r : Inner radius of rolled ring
H : Maximal radial thickness of rolled ring
B : Axial height of rolled ring
R_b : Radius of groove
S : Radial deepness of groove
B_b : Axial width of groove
ΔH : Reduction
Δh : Feed amount per revolution

References

[1] K. Davey and M. J. Ward, A practical method for finite element ring rolling simulation using the ALE flow formulation, *International Journal of Mechanical Sciences*, 44 (2002) 165-190.

[2] E. Eruc and R. Shivpuri, A summary of ring rolling technology - I. Recent trends in machines, processes and production lines, *International Journal of Machine Tools and Manufacture*, 32 (1992) 379-398.

[3] W. Johnson, I. MacLeod and G. Needham, An experimental investigation into the process of ring or metal type rolling, *International Journal of Mechanical Sciences*, 10 (1968)

455-468.

[4] J. B. Hawyard, W. Johnson and J. Kirkland, Analysis for roll force and torque in ring rolling with some supporting experiments, *International Journal of Mechanical Sciences*, 15 (1973) 873-893.

[5] A. G. Mamalis, W. Johnson and J. B. Hawkyard, Pressure distribution, roll force and torque in cold ring rolling. *Journal of Mechanical Engineering Science*, 18 (1976) 196-209.

[6] J. S. Ryoo, D.Y.Yang and W. Johnson, Ring rolling; the inclusion of pressure roll speed for estimating torque by using a velocity superposition method, In: *Proceedings of the 24th International MTDR Conference*, Manchester, 1983, 69-74.

[7] C. F. Lugora and A. N. Bramley, Analysis of spread in ring rolling, *International Journal of Mechanical Sciences*, 29 (1989) 132-140.

[8] D. Y. Yang and K. H. Kim, Rigid plastic finite element analysis of plain strain ring rolling, *International Journal of Mechanical Science*, 30 (1988) 571-580.

[9] N. Kim, S. Machida and S. Kobayashi, Ring-rolling process simulation by three dimensional finite element method, *International Journal of Machine Tools Manufacturing*, 30 (1990) 569-577

[10] S. G. Xu, J. C. Lian and J. B. Howkyard, Simulation of ring rolling using a rigid plastic finite elementmodel, *International Journal of Mechanical Sciences*, 33 (1991) 393-401.

[11] L. Hua and Z. Z. Zhao, The extremum parameters in ring rolling, *Journal of Materials Processing Technology*, 69 (1997) 273-276.

[12] F. L. Yan, L. Hua and Y. Q. Wu, Planning feed speed in cold ring rolling, *International Journal of Machine Tools & Manufacture,* 41 (2007) 1695-1701.

[13] L. G. Guo, H. Yang and M. Zhan, Research on plastic deformation behavior in cold ring rolling by FEM numerical simulation, *Modeling and Simulation in Materials Science and Engineering,* 13 (2005) 1029-1046.

[14] D. S. Qian, L. Hua and Z. J. Zuo, Investigation of distribution of plastic zone in the process of plastic penetration, *Journal of Material Processing Technology*, 187-188 (2007) 734-737.

[15] H. Yang, L. G. Guo and M. Zhan, Research on the influence of material properties on cold ring rolling processes by 3D-FE numerical simulation, *Journal of Materials Processing Technology*, 177 (2006) 634-638.

[16] P. V. Ranatunga, Modeling of profile ring rolling with upper bound elemental technique, PhD dissertation, The Ohio University, 2002.

[17] L. Hua, Z. J. Zuo and J. Lan, Research on following motion rule of guide roller in cold rolling groove ball ring, *Journal of Materials Processing Technology*, 187-188 (2007) 743-746.

[18] L. Hua, Z. J. Zuo and J. Lan, 3D finite element simulation and process design for cold rolling ball groove section ring, *Chinese Journal of Mechanical Engineering*, 44 (2008) 201-205.

[19] L. Hua, D. S. Qian and L. B. Pan, Analysis of plastic penetration in process of groove ball-section ring rolling, *Journal of Mechanical Science and Technology*, 22 (2008) 1374-1382.

[20] D. S. Qian, L. Hua and L. B Pan, Research on gripping conditions in profile ring rolling of raceway groove, *Journal of Materials Processing Technology*, 209 (2009) 2794-2802.

[21] D. S. Qian, Research on mechanical principle and technology design of profile cold ring rolling, PhD dissertation, Wuhan University of Technology, 2009.

[22] L. Hua, X. G.. Huang and C. D. Zhu, *Theory and Technology of Ring Rolling*, Chinese Machine Press, Beijing, 2001.

[23] A. E. Tekkaya, State-of-the-art of simulation of sheet metal forming, *Journal of Materials Processing Technology*, 103 (2000) 14-22.

[24] *Getting Started with ABAQUS*, 2003, Version 6.4, ABAQUS Inc., Pawtucket, USA.

[25] H. Yang and L. G. Guo, Effect of sized of forming rolls on cold ring rolling by 3D-FE numerical simulation, *Transactions of Nonferrous Metals Society of China*, 16 (2006) s645-s651.

[26] Z. X. Wang, *Conciseness Mechanical Design Manual*, Chinese Machine Press, Beijing, 1997.

[27] H. Yang, M. Wang and Z. C. Sun, 3D coupled thermo-mechanical FE modeling of blank size effects on the uniformity of strain and temperature distributions during hot rolling of titanium alloy large rings, *Computational Materials Science*, 44 (2008) 611-621.

Yu-Min Zhao, associate professor, teaching at School of Materials Science and Engineering, Wuhan University of Technology, specialize in research and developement of technology, mould and equipment of metal plastic forming.